Brookhaven Symposium Biol. 32
Brookhaven National Laboratory, June 1-4, 1982
NEUTRONS IN BIOLOGY, B. Schoenborn,
Plenum Press, NY

CONF-8206240--5

BIO 4086
BNL - 34674
Conf Art
Bk Chpt



BNL--34674

DE84 012173

# NEUTRON SCATTERING STUDIES OF THE H2a-H2b AND $(H3-H4)_2$ HISTONE COMPLEXES

R. Douglas Carlson

Brookhaven National Laboratory
Upton, NY 11973

## INTRODUCTION

The genetic information of higher organisms is contained, encoded along the nuclear DNA, in the chromatin, a fibrous complex of that DNA with protein and some RNA. Its basic structural unit, the nucleosome (34), is formed by the interaction of the DNA with a class of basic proteins, the histones. This subunit is repeated along the chromatin fibers like beads on a string. It represents the first in a series of levels of folding of chromosomal DNA within the nucleus.

The portion of the nucleosome that is highly conserved in all eukaryotes is the nucleosome core particle. It consists of a segment of about 145 base pairs of DNA wrapped around an octameric histone core comprised of two each of the four histones H2a, H2b, H3, and H4. The free core particle can be isolated after enzymatic cleavage of the connecting DNA. It has been shown to occupy a volume that is roughly a cylindrical disk, about 55 Å high and 110 Å in diameter (14,35,41). It is a common feature in all eukaryotes because its component histones are so highly conserved (20). These core particle histones can be dissociated from the DNA as an octamer in 2.0 M NaCl (42). At lower salt concentrations, the octamer further dissociates into an $(H3-H4)_2$ tetramer and two H2a-H2b dimers through a hexameric intermediate (13). Studies of the association between H3 and H4 and between H2a and H2b confirm that strong pairs are formed whether the histones are from the same species or whether histones from protozoa, fungi, plants, and vertebrates are mixed (10,34). Also, cross-linking studies show that these pair histones are in contact within chromatin (5,30). Together, these data suggest that the tetramers and

dimers exist in all eukaryotic chromatins and that their stuctural integrity is preserved within the nucleosome core particle.

Some information about the conformations of the pair complexes has already been established. Ultracentrifugation studies of the $(H3\text{-}H4)_2$ tetramer suggest that it has a very asymmetric conformation in solution (32,36). Proton NMR studies suggest that these complexes both have highly structured parts, with less structured N-terminal arms which are perhaps free to extend out into solution (32,33). A recent model for the tetramer, based on a low resolution image reconstruction analysis of electron micrographs of fibers of the octamer together with histone-histone and histone-DNA cross-linking data, is described as a "dislocated disk" or "dislocated horseshoe"—a disk-shaped object ~60 to 70 Å across, ~27 Å thick, and having a central hole (23). This model of the octamer suggests that the H2a-H2b dimer is an elongated structure, but no dimensions have been proposed.

Neutron scattering methods are used here for further study of the physical parameters such as size, shape, molecular weight, and volume of these complexes in solution. Additional information about the architecture of the H2a and H2b within the dimer is provided from studies of a complex formed by mixing undeuterated H2a with partially deuterated H2b from Euglena.

## MATERIALS AND METHODS

### Euglena Cell Cultures

Sterile cultures of Euglena gracilis (strain Z) were grown in heterotrophic acidic medium (17), stirred by having air sterilized by a line filter bubbled through it, in 9-liter bottles under a bank of cool-white fluorescent lamps (600 watts total). Euglena were also grown in Hutner's medium containing 80% $D_2O$ as a source of partially deuterated histones. Over a period of months, small (~50-ml) cultures in modified Erlenmeyer flasks were gradually adapted to tolerate increased levels of $D_2O$ in the medium by increasing the $D_2O$ concentration from 50% in steps of 5%. After adaptation, sufficiently vigorous growth was maintained in 80 or 85% $D_2O$ by bubbling sterile 1% $CO_2$ through ~600-ml cultures in one-liter culture flasks kept on a rotary shaker at 150 rpm to offset the cells' loss of natural motility at high levels of $D_2O$.

Cells were harvested by centrifugation when concentrations reached (1 to 2)x$10^9$ cells/liter. $D_2O$ levels in the media were maintained by measuring the IR absorption at 1.66 μm (9) on a Cary 14 spectrometer. The amount of deuterium incorporated into the histones was determined by measuring the proton NMR spectrum (31) on a Bruker WH-360 NMR spectrometer.

## Isolation of Chromatin

Chicken erythrocytes: The jugular vein of an adult chicken was cut, and the blood was collected in a beaker containing 1 ml heparin solution (500 units/ml). Nuclei were isolated by a procedure (47) that involves washing the erythrocytes three times with 0.34 M sucrose buffer A (15) to which 2 mM $Na_2EDTA$ (disodium ethylenediaminetetraacetic acid), 0.5 mM EGTA [ethyleneglycol-bis-(β-amino ethyl ether)-N,N'-tetraacetic acid], 0.5% Nonidet P40, and 0.1 mM PMSF (from 50 mM stock of phenyl-methyl-sulfonyl fluoride in isopropyl alcohol) have been added, and then three times with 0.34 M sucrose buffer A with 0.1 mM PMSF. Soluble chromatin was prepared either by digesting a nuclear suspension (50 $A_{260}$ units/ml) for 10 min at 37°C with 10 units/ml of micrococcal nuclease, or by disrupting nuclei washed with 0.2 M KCl by diluting ~100-fold with cold distilled water containing 0.1 mM PMSF (a protease inhibitor) and then homogenizing for 90 sec with a Virtis homogenizer at 0.9 full speed. SDS-polyacrylamide gel electrophoresis showed no differences between histones isolated by these two methods.

Euglena: Magnaval's procedure (27) for isolating nuclei from Euglena was modified to optimize the yield. Harvested cells were suspended in isolation buffer (10% sucrose, 10% Triton X-100, 10 mM Tris-HCl pH 7.4, 6 mM $MgCl_2$, 0.14 mM spermidine), then frozen (-40°C) and thawed three times. A suspension of about $5x10^7$ cells/ml was disrupted by using two strokes (1500 psi) of an Aminco French pressure cell. The pressate was washed at least three times with isolation buffer, and then centrifuged for 10 min at 1000 g. The pellet was resuspended to 1/3 the original volume with 2.0 M STM buffer (2.0 M sucrose, 10 mM Tris-HCl pH 7.4, 6 mM $MgCl_2$) and mixed thoroughly. Aliquots were layered on a step gradient containing equal volumes of 2.2 and 2.4 M STM buffer, the top interface was mixed, and the tubes were centrifuged at 23,000 rpm for 90 min in an SW25.2 rotor. The pellets (containing mostly nuclei and paramylon) were combined and washed in 0.25 M sucrose, 10 mM Tris-HCl pH 7.4, 0.1 mM PMSF, then resuspended in the same buffer to 1/10 the original volume. A crude soluble chromatin was prepared by disrupting the swollen nuclei with two strokes of the French press at 12,000 psi, Virtising the pressate for 60 sec at 0.9 full speed, and centrifuging for 10 min at 1000 g in order to pellet and remove the paramylon and other insoluble material.

## Isolation of Histone Complexes

Histone complexes were isolated by hydroxylapatite chromatography. Chicken H2a-H2b and $(H3-H4)_2$ complexes were isolated by the method of Simon (39) with 0.1 mM PMSF added to the buffers. Euglena complexes were isolated by a slightly modified form of this procedure used for purifying individual histones. After

dialyzing the soluble chromatin versus 0.5 M NP buffer (0.5 M NaCl, 0.1 M potassium phosphate pH 7.0, 0.1 mM PMSF), most of the H1 was removed by mixing the chromatin with AG50W X-2 resin for one hour at 4°C (4). The chromatin was then mixed with an amount of hydroxylapatite sufficient to bind all of the DNA, and a column was poured from the slurry. A large amount of nonhistone protein is eluted with the 0.5 M NP buffer. The NaCl in the eluting buffer is then increased to 1.0 M, and the H2a-H2b complex is eluted along with some remaining H1-like protein. (The Euglena H1 dissociates from the DNA at roughly the same NaCl concentration as does the H2a-H2b complex.) Following a linear gradient to 1.2 M NP buffer, the $(H3\text{-}H4)_2$ is eluted with 2.0 M NP buffer.

## Histone Purification

The individual H2a and H2b histones were isolated by gel filtration chromatography. The H2a-H2b fractions from the hydroxylapatite columns were added to long (1.5- to 1.8-m) Biogel P-60 columns. The elution buffer used to separate the H2a and H2b from chicken was 0.02 M HCl, 0.05 M NaCl, 0.02% $NaN_3$ (43). The elution buffer for H2a and H2b from Euglena was 0.02 M HCl and 0.02% $NaN_3$. The H2a and H2b were eluted as separate peaks. The peak fractions were pooled to eliminate cross-contamination, and their purity was monitored by SDS-polyacrylamide gel electrophoresis. In some cases, pools were rechromatographed for additional purification.

## Complex Formation

Purified H2a and H2b (deuterated or undeuterated) from Euglena were mixed to form the H2a-H2b dimer under conditions chosen to minimize the formation of aggregates (1,19). Dilute ($\sim 10^{-5}$ M) equimolar solutions of H2a and H2b in cold 1 mM HCl were mixed, then dialyzed versus 10 mM sodium phosphate, 0.25 mM EDTA, 0.1 mM DTT (DL-dithiothreitol), pH 7.0 (1). The mixture was then extensively dialyzed versus 2.0 M NaCl, 10 mM Tris-HCl, 0.25 mM EDTA, 0.1 mM DTT, 0.1 mM PMSF, pH 7.5.

## Neutron Scattering Samples

All complexes, whether isolated directly from chromatin by hydroxylapatite chromatography or formed by mixing the purified histones, were concentrated in an Amicon stirred ultrafiltration cell with a PM 10 membrane and run on a long 1.5 x ~170-cm Sephadex G100 column equilibrated with scattering buffer (10 mM Tris-HCl pH 7.5, 0.25 mM NaEDTA, 0.1 mM DTT, 0.1 mM PMSF, and either 0.2 M or 2.0 M NaCl) to ensure that only the appropriate dimer or tetramer forms were present in the scattering sample. The formed complexes generally showed a large peak with a small leading edge, and the fractions were pooled accordingly. In all cases, the pooled peak fractions were concantrated and dialyzed

extensively with several buffer changes versus scattering buffer made with either $D_2O$ or $H_2O$. The contrast match-point measurements to determine the match-points of the complexes were made in $H_2O$ and $D_2O$ buffers and in two intermediate buffers as well. These latter samples were prepared for the undeuterated chicken complexes by mixing portions of the $H_2O$ and $D_2O$ samples. Precision positive displacement micropipettors (Scientific Manufacturing Industries) were used to measure out the appropriate volumes of each. Identical procedures were followed for samples and buffers. The intermediate Euglena H2a-H2b samples were prepared by dialyzing ~0.3 ml of sample versus the appropriate buffer for at least two days. The dialysate served as the buffer for scattering measurements.

All samples were monitored before and after the scattering experiment by measuring the $A_{275.5}$ directly in the quartz sample cells. Weight concentrations for chicken histone solutions were obtained from molar extinction coefficients at 275.5 nm (10) and molecular weights determined from the amino acid sequences (7,25,44,45). Molar extinction coefficients used for Euglena H2a and H2b were determined from $A_{275.5}$ measurements made on a Cary 219 spectrometer, amino acid composition measurements made with a Beckman 890C sequencer, and molecular weights that were estimated from SDS-polyacrylamide gels.

## Neutron Scattering Measurements

Neutron scattering experiments were conducted at the H4-S low-angle spectrometer (38) and the more recently completed H9 cold-moderated low-angle spectrometer (37) in the High Flux Beam Reactor at Brookhaven National Laboratory. Scattering experiments on undeuterated histone complexes from chicken were conducted at H4-S. Sample-to-detector distances varied from 160 to 198 cm in separate experiments, and the nominal wavelength $\lambda$ varied from 2.33 to 2.36 Å ($\Delta\lambda/\lambda$ = 0.02 full width at half maximum). Collimation was by two cadmium disks with circular apertures 6 mm in diameter, 1.4 m apart. Scattering experiments on partially deuterated and undeuterated histone complexes from Euglena were conducted at H9. The sample-to-detector distance was 109.7 cm, and the nominal wavelength was 4.98 Å ($\Delta\lambda/\lambda$ = 0.08 FWHM). Collimation was by four cadmium apertures 10, 8, 6, and 5.5 mm in diameter, spaced over a distance of 1.6 m. Samples were contained in 2- or 3-mm-thick quartz cuvettes. Cells were mounted in an automatic sample changer that was kept at 6°C during the experiments. Sample and buffer cells were repeatedly exposed to the beam in a sequential fashion, with data collected for a preset number of monitor counts (the incident beam intensity is constantly monitored by a low efficiency detector) to minimize the effects of beam fluctuations, variations in the background, and sample changes. Data were also collected for an empty cell, for a sample

cell containing 8% $D_2O$ (an incoherent scatterer), and with the beam blocked. Sample integrity was monitored by measuring the UV absorbance and by SDS-polyacrylamide gel electrophoresis, before and after each experiment.

Scattering intensities were measured by a two-dimensional position-sensitive detector (38) that encodes the positions of the detected neutrons, summing them into elements of a 128 x 128 array. Data from repeated runs on a given sample were summed together and radially integrated, and the counts per unit area in successive annular rings were calculated to give the scattered intensity as a function of Q, the amplitude of the scattering vector, where $Q = 4\pi(\sin\theta)/\lambda$, $2\theta$ is the scattering angle, and $\lambda$ is the neutron wavelength. These data were scaled to a fixed number of incident beam monitor counts and divided through by the incoherent scattering profile to eliminate detector non-uniformities. A general expression for obtaining the solute scattering profile I(Q) is

$$I(Q) = [I_1(Q) - I_4(Q)]/T_1 - (1 - \bar{v}c)[I_2(Q) - I_4(Q)]/T_2 - (\bar{v}c)[I_3(Q) - I_4(Q)]/T_3 \quad (1)$$

where $\bar{v}$ is the partial specific volume (assumed to be 0.74 for histone complexes), c is the weight concentration of the solute, and the I's represent the scattered intensities and the T's the fractions of the incident beam transmitted by a given sample (subscript 1), buffer (subscript 2), and the empty cell (subscript 3). The background intensities, $I_4$, were determined by blocking the incident beam. They were small enough to be neglected at H4-S but not H9.

## Data Analysis

The radii of gyration, R, of the solute molecules were determined from small-angle scattering data for those angles for which the Guinier approximation holds. In this angular region

$$I(Q) = I(0) \exp(-R^2Q^2/3) \quad (2)$$

and R is determined from the slope of the least-squares fit of the $\ln[I(Q)]$ vs $Q^2$ data, but I(0) is determined by extrapolating the linear plot to $Q^2 = 0$. Because the scattering length density of a solute particle is usually not uniform, R depends on the contrast $\bar{\rho}$, the difference between the mean scattering length density of the particle and that of the solvent. This relationship can be expressed in a general way (18):

$$R^2 = R_c + a/\bar{\rho} - b/\bar{\rho}^2 \quad (3)$$

where $R_c$ is the radius of gyration at infinite contrast, and a and b are constants, the magnitude of a depending on the radial variation of the scattering length density, and that of b on the dependence of the contrast on the separation between the particle's center of volume and center of scattering length density. It follows that I(0) is also dependent on the contrast between the solvent and the particle. It can be shown that

$$I(0)/C \propto \rho_s^2 \tag{4}$$

where C is the solute concentration and $\rho_s$ is the scattering length density of the solvent. At the point where the solvent scattering length density equals the means scattering length density of the particle, I(0) vanishes as the particle is contrast matched. This contrast match-point can be determined by plotting $[I(0)/C]^{1/2}$ vs the percent $D_2O$ in the buffer. At the match-point, the dry volume of the particle is

$$V = \Sigma b_i/\rho_s \tag{5}$$

where the $b_i$'s are the scattering length densities of all the atoms in the particle. If the amino acid composition of a protein is known, then $\Sigma b_i$ can be calculated (21), and V can be determined. The contrast dependent scattering data can also be used to calculate the molecular weight, M, of the particle according to the relationship (46)

$$\frac{\partial[I(0)/C]^{\frac{1}{2}}}{\partial\beta} = \left(\frac{\Phi_o AZ\Delta\Omega}{N_A}\right)^{\frac{1}{2}} \bar{v}M^{\frac{1}{2}} \left(\frac{\partial\bar{\rho}}{\partial\beta}\right) \tag{6}$$

where C is the solute concentration, $\bar{v}$ is the partial specific volume, and $\beta$ is the volume fraction of $D_2O$ in the solvent. The term involving $\Phi_o$ (the incident neutron flux), A (the cross-sectional area of the beam at the sample), Z (the sample thickness), $\Delta\Omega$ (the solid angle of the detector), and $N_A$ (Avogadro's number) is required to put the data on an absolute scale.

## Model Calculations

Models were evaluated on the basis of their calculated scattering profiles, radii of gyration, and volumes. By plotting I/I(0) versus QR, where R was determined from the Guinier region of the profile, the effect of particle size is factored out. In the angular region of interest for these experiments, this scattering profile then reflects primarily the shape of the particle. It is thus reasonable to use solid, uniform density models as a first approximation in searching for the particle shape (2,24). How well a model profile agrees with the experimental data is a measure of how well that model approximates the shape of the

complex in solution. Many types of models can be quickly eliminated on the basis of shape. Once a model is found that gives good agreement in this shape region of the scattering profile, information about size is put back in to see whether it can have a volume and a radius of gyration that are also consistent with the experimental results.

Spherically averaged scattering profiles for certain uniform density models such as oblate and prolate ellipsoids, cylinders, disks, and disks with a central hole were found in the literature. Calculations for other models, including some in which the shape and/or density is irregular, were made with a program that divides the structure into a cubic array of equal-volume scattering elements (typically 3000) and uses the coordinates of the center of each element to calculate the spherically averaged scat-

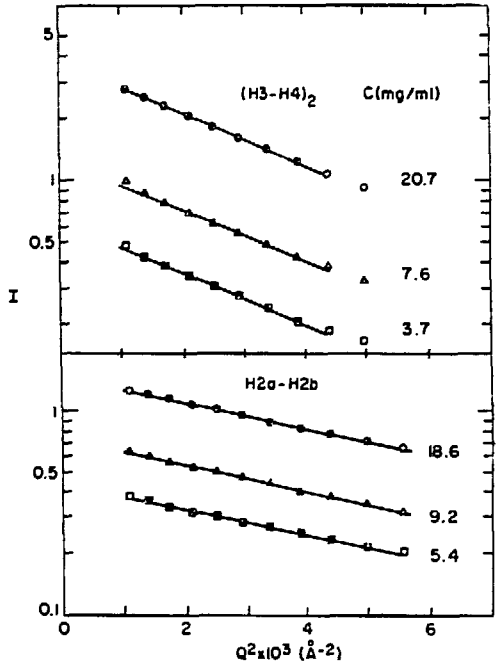


Fig. 1. Guinier plots obtained for different concentrations of $(H3-H4)_2$ tetramers and H2a-H2b dimers from chicken chromatin in 0.2 M $D_2O$ scattering buffer showing no significant concentration dependence. The radii of gyration determined from fitting the solid data points with use of a linear regression were, in order of decreasing sample concentration: for $(H3-H4)_2$, 29.6, 29.3, and 29.6 Å; for H2a-H2b, 21.0, 20.8, and 20.6 Å.

tering profile from the Debye relationship (11). For the dislocated disk or lockwasher models, a program to generate the coordinates for a disk with a central hole was modified so that a helical rise produces a dislocation at the origin. A gap at one end can be produced by defining a range of angles for which the array element does not exist. Radial variations in the scattering length density are produced by varying the scattering length densities assigned to the array elements.

## RESULTS

Neutron scattering data were collected during several experiments on the H2a-H2b and $(H3\text{-}H4)_2$ histone complexes from chicken erythrocyte chromatin. These data are presented in Figures 1 to 4 and 6 and Table 1. Guinier plots of the scattering data for each complex at different sample concentrations in $D_2O$ buffers are shown in Figure 1. Only the linear regions of the scattering profiles are shown. The slopes, shown as continuous lines, were determined by linear least-squares regressions. They do not change significantly as the concentration is increased. Data collected on H2a-H2b and $(H3\text{-}H4)_2$ samples at still lower concentrations of 1.5 and 2.1 mg/ml, respectively, also support this conclusion, although the statistical variance of the data was greater. Thus interparticle interference effects and aggregration are not significant in this buffer over this concentration range.

Figures 2 and 3 show Guinier plots of data obtained for these complexes in different contrast buffers. The data show, as expected, very little variation in R as the $D_2O/H_2O$ ratio changes. The radii of gyration determined from several separate experiments in $D_2O$ buffer were 21.0±0.4 Å for H2a-H2b and 28.8±0.6 Å for $(H3\text{-}H4)_2$. The forward scattering intensity, I(0), in each buffer was determined by extrapolating the linear least-squares fit of the data to $Q^2 = 0$. Figure 4 shows how the I(0)'s are used to determine the contrast match-points (the $D_2O$ percentages at which $I(0) \to 0$) for each complex. These were 41.9±0.2% $D_2O$ for the dimer and 40.9±0.6% $D_2O$ for the tetramer. From the amino acid sequences of the core histones (7,25,44,45), the number of exchangeable hydrogens in each amino acid (21), and the observation via infrared spectroscopy that all these labile hydrogens in chromatin exchange except for about 40% of those in the amide (NH) groups (16), the total scattering length ($\Sigma b_i$) of each histone complex at the $D_2O/H_2O$ mixture corresponding to the match-point has been calculated. Use of these results to calculate dry volumes by using Eq. (5) gave $3.30 \times 10^4$ Å$^3$ for the dimer and $6.56 \times 10^3$ Å$^3$ for the tetramer. These are compared in Table 1 with volumes calculated by summing the volumes of individual amino acids (21). The data in Figure 4 were also used, together with the calculated variation in contrast of the protein with $D_2O$ percent, with exchangeable

hydrogens taken into account, to calculate the molecular weights of the complexes by Eq. (6). Values of 28,200 daltons for the dimer and 61,100 daltons for the tetramer are compared in Table 1 with molecular weights calculated from the amino acid sequences. The calculations confirm that these samples were in fact the H2a-H2b dimer and the $(H3\text{-}H4)_2$ tetramer, not larger complexes or aggregates.

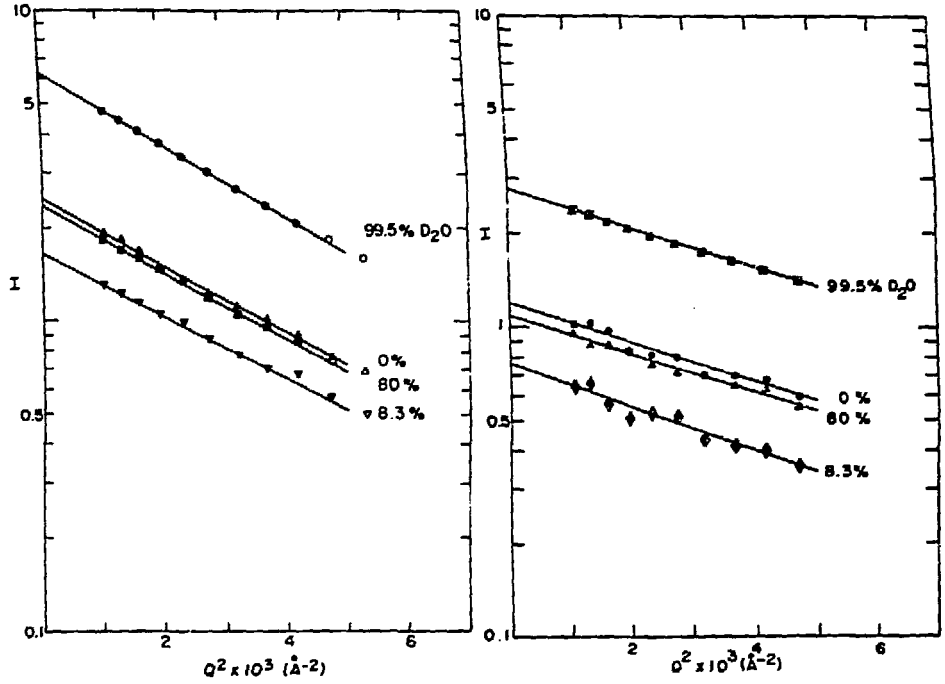


Fig. 2. (Left) Contrast dependent scattering data for $(H3\text{-}H4)_2$ tetramers as a function of the $D_2O$ percentage in 0.2 M scattering buffer. Sample concentrations varied from 14.0 to 16.0 mg/ml.

Fig. 3. (Right) Contrast dependent scattering data for H2a-H2b dimers as a function of the $D_2O$ concentration in 0.2 M scattering buffer. Sample concentrations varied from 12.4 to 15.3 mg/ml.

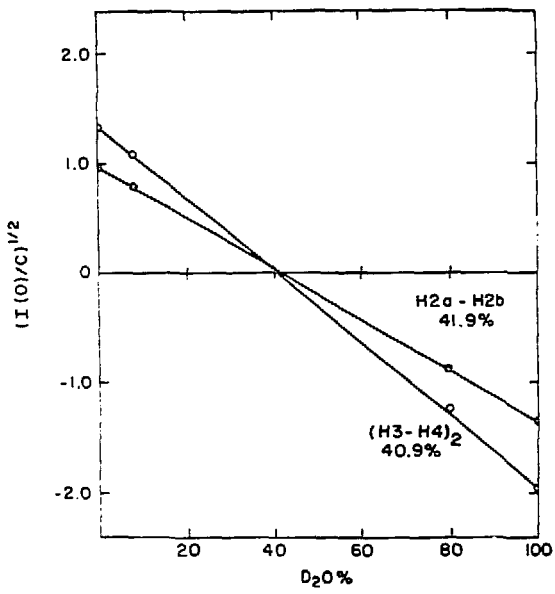


Fig. 4. Determination of the contrast match-points for the $(H3-H4)_2$ and H2a-H2b complexes from forward scattering data obtained by extrapolating the Guinier regions of Figures 2 and 3 to $Q^2 = 0$.

Table 1. Scattering Data for the $(H3-H4)_2$ and H2a-H2b Complexes from Chicken Erythrocytes

| Measured parameter | $(H3-H4)_2$ | H2a-H2b |
|---|---|---|
| Radius of gyration ($D_2O$ buffer) | 28.8±0.6 Å (4 expts.) | 21.0±0.4 Å (6 expts.) |
| Match-point | 40.9±0.6% $D_2O$ ($\rho = 2.28\times10^{-14}$ Å/cm$^3$) | 41.9±0.2% $D_2O$ ($\rho = 2.35\times10^{-14}$ Å/cm$^3$) |
| Volume | $6.56\times10^4$ Å$^3$ | $3.30\times10^4$ Å$^3$ |
| Calculated* | $6.79\times10^4$ Å$^3$ | $3.56\times10^4$ Å$^3$ |
| Molecular weight | $6.11\times10^4$ daltons | $2.82\times10^4$ daltons |
| Calculated* | $5.32\times10^4$ daltons | $2.78\times10^4$ daltons |

*Calculated, by summation, from the amino acid composition and the individual amino acid volumes.

The extended scattering profiles for these two complexes, together with several representative profiles calculated for some of the models in Figure 5, are shown in Figure 6. Comparison of the $(H3\text{-}H4)_2$ tetramer data with various model profiles led to the conclusion that the tetramer is extremely flattened in solution. The shape of the scattering profile is not consistent with less asymmetric structures or with elongated structures. Of the models

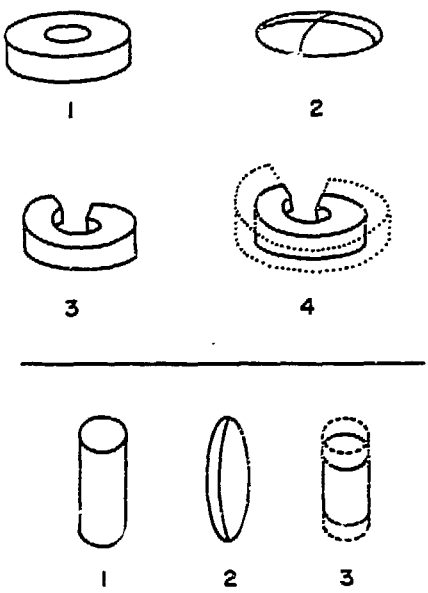


Fig. 5. Some representative models for which scattering profiles have been compared with the experimental profiles. Four types of $(H3\text{-}H4)_2$ models are shown (top): 1) hollow disks, for which the thickness and the inner and outer diameters were varied, 2) oblate ellipsoids with different axial ratios, 3) a dislocated disk or lockwasher based on the model of Klug et al. (23), for which the inner and outer diameters, thickness, amount of dislocation, and presence or absence of a gap on one side were varied, and 4) a dislocated disk surrounded by a shell of lower scattering length density, for which the scattering length density and diameter of the shell were varied. Three H2a-H2b models are shown (bottom): 1) right circular cylinders with different length/diameter ratios, 2) prolate ellipsoids with different axial ratios, and 3) cylinders with lower scattering length density "tails" at each end, for which the length, diameter, and scattering length density were varied.

considered, only very flattened structures give a reasonable fit. The extreme asymmetry in the tetramer is demonstrated in Figure 6 by the good agreement over most of the angular range for which data were collected between the experimental data and profile 3, the calculated profile of a uniform oblate ellipsoid of axial ratio 1:5. Other flattened solids such as cylindrical disks and disks with holes in the center also give this kind of agreement with the data only when the axial ratio is that great. Profiles 1 and 2 were calculated for irregular-shaped models based on a tetramer model proposed after evaluation of a low resolution image

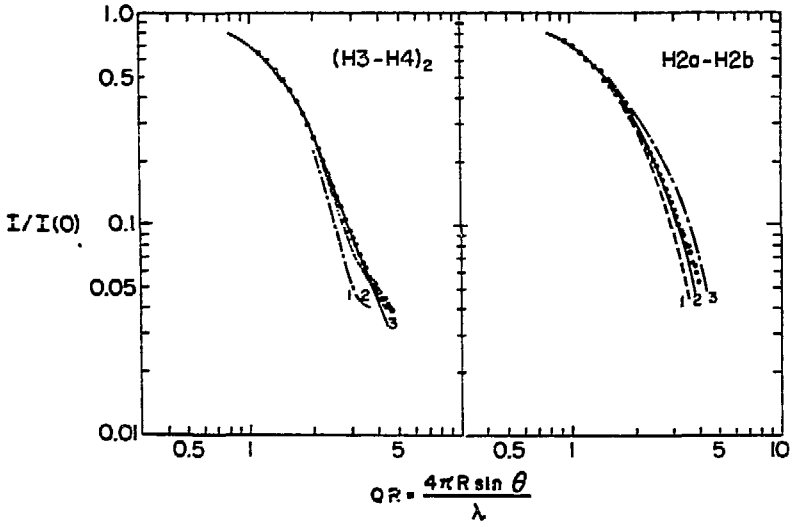


Fig. 6. Experimental scattering data for the $(H3\text{-}H4)_2$ and H2a-H2b complexes (points) compared with selected model calculations. See text for further discussion of the models. The $(H3\text{-}H4)_2$ data are shown with calculated profiles for 1) a dislocated lockwasher (Figure 5-3 top) with inner diameter = 24 Å, outer diameter = 66 Å, thickness = 27 Å, dislocation (over 360° rotation) = 13.5 Å, and gap = 24 degrees; 2) a dislocated lockwasher plus shell model (Figure 5-4 top) with inner diameter = 24 Å, outer diameter = 64 Å, shell diameter = 96 Å, thickness = 18 Å, dislocation (over 360° rotation) = 18 Å, gap = 24 degrees, and ratio of the scattering length density of shell to that of core = 0.21; 3) an oblate ellipsoid of axial ratio 1:5 (Figure 5-2 top). The H2a-H2b data are shown with calculated profiles for uniform cylinders with different length/diameter ratios (v) (Figure 5-1 bottom): 1) v = 2.0; 2) v = 2.37; 3) v = 3.0.

reconstruction of the histone octamer together with various histone cross-linking data (23). Profile 1 is a model calculation for a dislocated disk, or lockwasher, with a gap at one end, and with dimensions that approximate those of the proposed tetramer model as it has been described. The radius of gyration, determined from the Guinier region of the scattering profile, was 26.4 Å and the volume was $7.48 \times 10^4$ Å$^3$, quite different from those values determined from the experimental profile. Also, the calculated profile falls off much too quickly with Q. Small adjustments of the model dimensions do not significantly lessen the lack of agreement between the data and the model profile. Very similar results were obtained for other calculations with or without a gap and with dislocations varying between 0 and 27 Å. To improve the agreement with experimental results, a more flattened model is required. Profile 2 represents a calculation for a similar dislocated disk model that has been surrounded by a shell of lower scattering length density chosen to approximate the spatial averaging of free N-terminal tails of the H3 and H4 extending outward into solution (6) from the globular core represented by the dislocated disk. The agreement between the observed and calculated scattering profiles is greatly improved. The radius of gyration, 29.4 Å, is also closer to that determined experimentally, as is the volume, $6.50 \times 10^4$ Å$^3$.

The neutron scattering data suggest that the H2a-H2b dimer is also quite asymmetric in solution, but, unlike the $(H3\text{-}H4)_2$ tetramer, it has an elongated structure. No model has been found that can be considered to uniquely agree with the data. Instead, several different types of elongated models can be shown to agree almost equally well with the data. For each type, the best dimensions have been determined by comparing the experimental and model profiles, volumes, and radii of gyration. Figure 6 shows the extended H2a-H2b scattering profile plotted along with model calculations for three representatives of one of these model types, a uniform density right circular cylinder, differing in their axial ratio (v). Of the three, the best match to the shape scattering is observed for a cylinder with v = 2.37 (profile 2). Converting this into particle dimensions of 64 Å length and 27 Å diameter gives a radius of gyration of 20.8 Å and a volume of $3.61 \times 10^4$ Å$^3$, values in good agreement with the experimental values. A slightly longer 83-Å x 30-Å prolate ellipsoid (profile not shown) fits the shape region almost as well, with a radius of gyration of 20.8 Å and a volume that is still larger by about 10%, $3.91 \times 10^4$ Å$^3$. A third type of elongated model, a cylinderical core with lower scattering density tails at either end, can also fit the data quite well. These lower density regions were chosen to approximate the average positions of N-terminal arms of the H2a and H2b extending out from a globular core with considerable freedom to move or flop around in solution. For example, a core-tail model 90 Å long and 27 Å in diameter, with a 50-Å-long core sandwiched

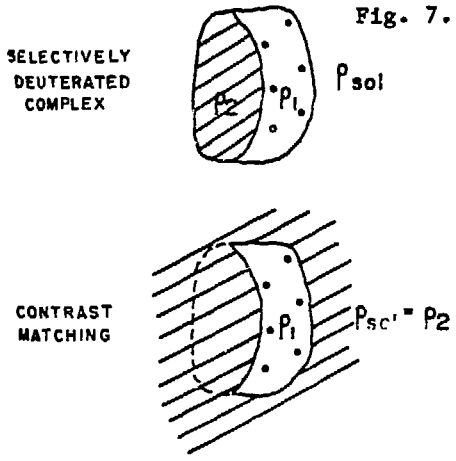


Fig. 7. Schematic representation of a contrast variation experiment in which a portion of a reconstituted protein complex is deuterated and a portion is not. By adjusting the scattering length density of the solvent, $\rho_{sol}$, to equal the scattering length density of the undeuterated part, $\rho_2$, that part can essentially be "matched out."

between two 20-Å tails having scattering length densities 1/5 of that in the core (profile not shown), fits the shape region almost as well as the 64 x 27-Å cylinder, dropping off a little faster after $QR > 2.5$, with a radius of gyration of 21.1 Å and a volume of $3.78 \times 10^4$ Å$^3$. Because each of these generally similar models agrees almost equally well with the data, no one of them is eliminated. It should be emphasized, however, that, of the models examined, only elongated models are consistent with the data.

Further information about the relative conformations of the individual histones within a complex can be obtained if sufficient scattering contrast between them can be produced, as shown schematically in Figure 7. An attempt was made to do this by reconstituting the H2a-H2b dimer with undeuterated H2a and partially deuterated H2b from Euglena. The amount of deuterium incorporated at nonexchangeable positions in a total histone fraction isolated from Euglena cultures grown in 80% $D_2O$ Hutner's medium (see Materials and Methods), measured by comparing the proton NMR spectra of the partially deuterated histone and of undeuterated histone (31), was found to be 50.7±5%. The uncertainty is an estimate based on the uncertainties in determining the base line, integrating the spectra, and determining the relative sample concentrations from amino acid analyses. This partially deuterated histone will be referred to as 50% deuterated histone.

Figure 8 shows scattering data collected for the H2a-H2b dimer formed by mixing the undeuterated Euglena H2a with 50% deuterated H2b, designated $(H2a)_H$-$(H2b)_D$. From the forward scattering data the match-point was found to be 65.2±1.3% $D_2O$ (Figure 9). With the known amino acid sequences of chicken H2a and H2b (25,44) used as an approximation since the Euglena

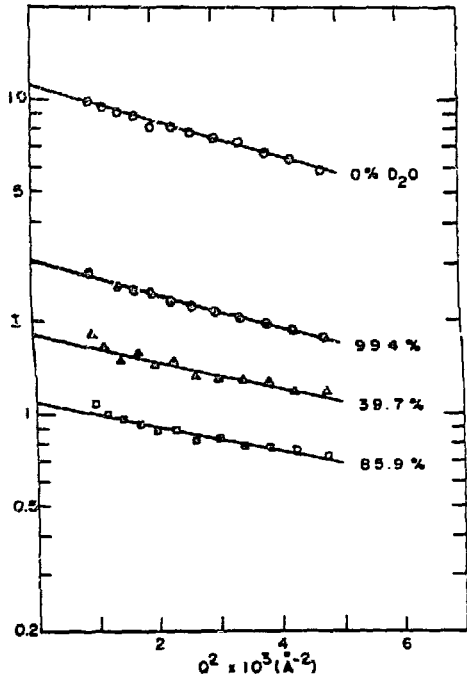


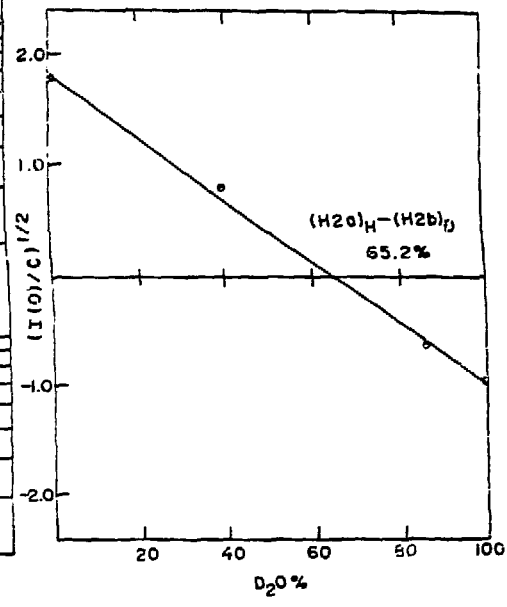


Fig. 8. (Left) Contrast dependent scattering data for the $(H2a)_H-(H2b)_D$ complex reconstituted from Euglena histones. The $D_2O/H_2O$ ratio of the 2.0 M scattering buffer was varied. Sample concentrations ranged from 11.6 to 13.7 mg/ml.

Fig. 9. (Right) Determination of the contrast match-point for the $(H2a)_H-(H2b)_D$ complex by plotting I(0)'s obtained by extrapolating the Guinier regions of Figure 8 to $Q^2 = 0$.

sequences are not known, the experimental volume of $3.30 \times 10^4$ Å$^3$ used for the chicken dimer, and the H2b assumed to be 50% deuterated, a match-point of 90% $D_2O$ for H2b alone and 67% $D_2O$ for $(H2a)_H-(H2b)_D$ has been calculated. This suggests that the amount of deuteration of the Euglena H2b is close to that determined for the whole histone.

Figure 10 shows a Stuhrmann plot, comparing the contrast dependence of the radii of gyration determined in Figures 3 and 8 for undeuterated chicken H2a-H2b and for the Euglena $(H2a)_H-(H2b)_D$ complexes. The measured radius of gyration for a completely undeuterated Euglena dimer sample in $D_2O$ buffer was 20.4 Å. The predominant feature of this plot for the partially deuterated

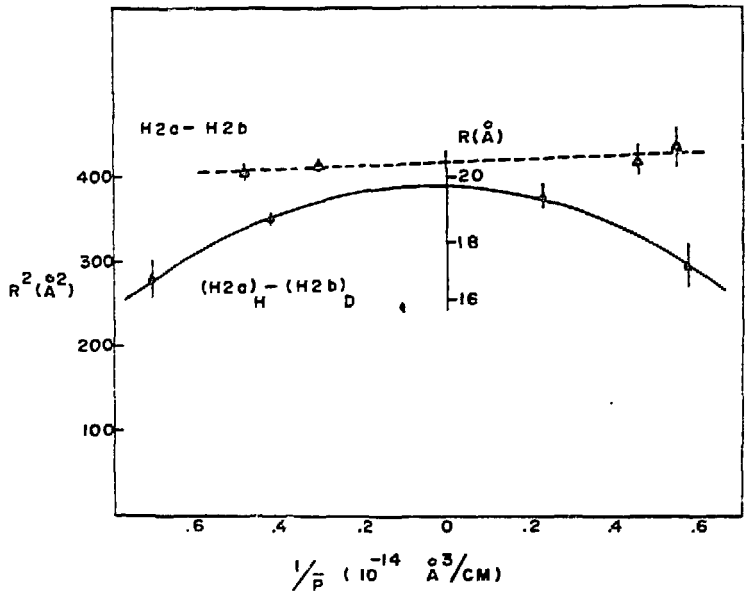


Fig. 10. Stuhrmann plot of the variation of the square of the radius of gyration of the undeuterated H2a-H2b complex from chicken (see Figure 2) and the $(H2a)_H$-$(H2b)_D$ complex from Euglena (see Figure 8) as a function of inverse contrast. A linear least-squares fit of the data for the undeuterated complex (dashed line) is shown along with a least-squares fit of the $(H2a)_H$-$(H2b)_D$ data to the quadratic equation

$$R^2 = R_o^2 + a(1/\bar{\rho}) - b(1/\bar{\rho})^2, \text{ where}$$

$R_o$ = 19.7 Å, a = $-1.92 \times 10^{-5}$, and b = $2.54 \times 10^{-10}$ $Å^{-2}$.

dimer is its curvature. It indicates that the center of mass of the undeuterated part and that of the 50% deuterated part of the dimer are not concentric. A least-squares fit of the data to a quadratic equation of the form of Eq. (3) is plotted along with the data points. From the coefficient b, the contrast between the deuterated and undeuterated parts (calculated from the match-points of the mixed complex), and their estimated volume ratios, the centers of mass of the undeuterated and deuterated parts are calculated (46) to be 20 Å apart.

The extended scattering curves for the undeuterated and partially deuterated complexes in their highest contrast buffers (see Figures 3 and 8) are compared in Figure 11. The chicken H2a-H2b data in $D_2O$ buffer are shown together with the Euglena $(H2a)_H$-$(H2b)_D$ data in $H_2O$ buffer. The reasonably good agreement, al-

though the contrast in the partially deuterated complex is less, verifies that, at least at low resolution, the shapes of the two complexes are similar. The scattering by the $(H2a)_H$-$(H2b)_D$ at a $D_2O/H_2O$ ratio near the match-point of the undeuterated H2a is shown in Figure 12. Here the scattering is contributed primarily by the deuterated H2b. The statistics are limited because of the relatively low contrast between the buffer and the $(H2b)_D$ and because the mass concentration of H2b is about half that of the complex as a whole. Nevertheless, the data suggest that the H2b is at least as asymmetric as the dimer.

## DISCUSSION

It seems likely that histone organization within the nucleosome core particle in all eukaryotes is essentially identical. The

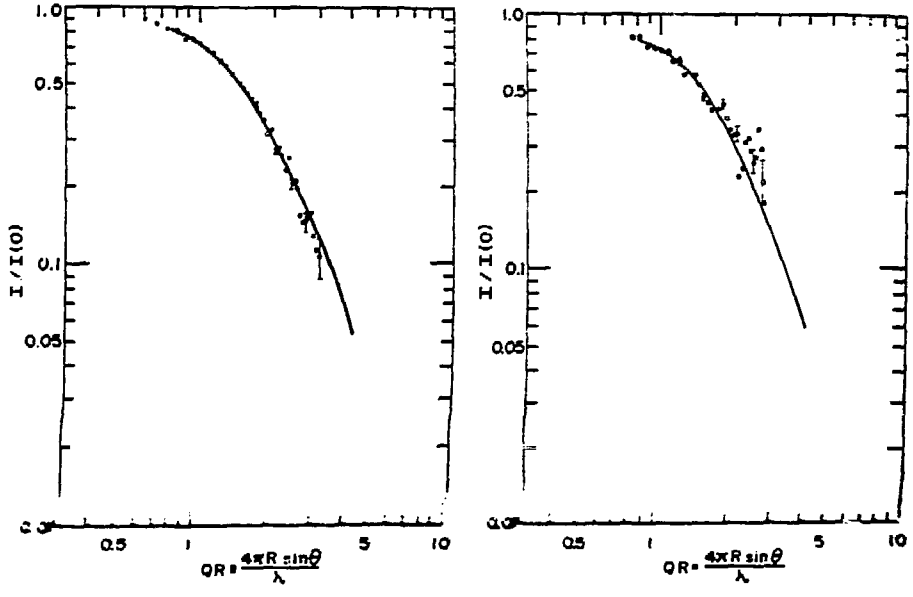


Fig. 11. (Left) Comparison of the normalized scattering profiles for undeuterated chicken H2a-H2b in 0.2 M $D_2O$ scattering buffer (solid line; representation of the experimental data in Figure 6) and Euglena $(H2a)_H$-$(H2b)_D$ in 2.0 M $H_2O$ scattering buffer (dots).

Fig. 12. (Right) Comparison of the normalized scattering profiles for undeuterated chicken H2a-H2b in 0.2 M $D_2O$ scattering buffer (solid line) and Euglena $(H2a)_H$-$(H2b)_D$ (dots) in 2.0 M scattering buffer containing 39.7% $D_2O$.

core particle is a highly conserved feature of all eukaryotic chromatins as are the primary sequences of the individual histones. The specific histone-histone interactions are apparently the same in different species, the association properties of mixed histone pairs from very different species are essentially identical, and the octamers from different species can be dissociated into dimer and tetramer pairs. It thus seems likely that information about the conformations of the H2a-H2b dimer and the $(H3\text{-}H4)_2$ tetramer complexes from both chicken and Euglena in solution will help elucidate how these histones are arranged within the octamer core of the nucleosome core particle.

It appears that the unusually asymmetric distribution of charged amino acids in the individual histones results in an unusual structural feature of the histone complexes. In general, the N-terminal regions of each polypeptide chain are highly basic (20). These complexes have been shown, by proton NMR studies, to have spectra very different from those of completely globular proteins (32,33). Spectra of association products of histone fragments indicate that the N-terminal segments are not highly structured and are primarily responsible for these spectral differences. These segments are apparently not necessary for complex formation, and are accessible for enzymatic or chemical cleavage (3). They are thought either to be loosely bound or to extend from the globular part of the complexes as free arms. If these arms are loosely bound on the outside of the structure, then the complex would appear to be fully globular. If, however, they do extend out from the globular part and are free to move, they would contribute more substantially to the radius of gyration and shape scattering profile of the complex. The extended neutron scattering profiles of the dimer and tetramer complexes from chicken erythrocytes show that both are quite asymmetric. The dimer is an elongated structure, and the tetramer is a flattened or oblate structure. Comparison of the experimental profiles with calculated profiles for various models suggests the approximate shapes of the complexes. Data on the radius of gyration and volume aid in further defining the dimensions and in eliminating certain models. They also suggest where the N-terminal arms might be located. They are not sufficient, however, to provide unique structural solutions.

Comparison of the scattering profile for the $(H3\text{-}H4)_2$ tetramer with various model profiles suggests that a significant percentage of the total scattering length of the complex must be located at a distance >30 Å from its center to account for its large radius of gyration. The tetramer must certainly be much thinner than the core particle or octamer (~55 Å), and it appears that it must extend out beyond the ~35-Å radius of the core particle model that has been suggested (23). The amount of asymmetry is indicated by the good agreement between the experimental pro-

file in Figure 6 and the calculated scattering profile for an oblate ellipsoid with an axial ratio of 1:5. Such an ellipsoid with a major axis of 90 Å and a minor axis of 18 Å has a radius of gyration of 28.7 Å, in excellent agreement with the observed value, and a volume of $7.63 \times 10^4$ Å$^3$, about 15% too large. Changing the dimensions to reduce the volume would of course also reduce the radius of gyration. The agreement is good enough to suggest that, with slight modifications, the fit could be improved.

If the solution structure corresponds fairly closely to that found in the octamer, then a possible explanation for the apparent discrepancy in these data is that the asymmetry of the tetramer is increased by the N-terminal arms extending radially outward from the complex, roughly in the flattened plane of the particle. It is easy to see how this would contribute to the large frictional coefficient previously observed in hydrodynamic studies (32,33), and to such a large radius of gyration. Figure 6 shows that by incorporating the basic features of the tetramer model suggested by Klug and others (23), for example, making the complex about 18 to 20 Å thick instead of 27 Å and extending its diameter to ~100 Å by putting a lower density shell around it to approximate the effect on the scattering that freely moving arms would have, the agreement with the data is much improved. At low resolution, the overall shape of this more detailed model is similar to that of the 1:5 oblate ellipsoid. It is the details of the model that are responsible for producing the structure in the model profile that is present in the experimental profile. Reducing the thickness not only increases the asymmetry as required, but it also reduces the volume of the globular core by an appropriate amount to allow for putting about 25% of the total volume of the tetramer in the free arms. The image reconstruction of the octamer does not show arms extending outward, but the arms would not be expected to show up, by the very nature of the technique, if they move freely. A more detailed description of the complex is not possible at this time. Further clarification of the relative structures of the arms and the globular part of the tetramer is likely to come from comparison of these data with those obtained for tetramers whose N-terminal arms have been enzymatically cleaved (26). An attempt by us to measure their scattering profile in 0.2 M scattering buffer was unsuccessful because of problems with aggregation.

As has been discussed, several types of elongated structures have been considered to explain the scattering by the H2a-H2b dimer. Only elongated models are able to explain the data. The combined radius of gyration, volume, and shape data are quite consistent with a circular cylinder 27 Å in diameter and 64 Å long, long enough to approximately span the octamer. However, a slightly longer prolate ellipsoid or a cylinder with ends having lower scattering length density to approximate the spatial averaging of free arms can also give good agreement with the data. No

effort was made to apply statistical tests to determine which of these models gave the best fit to the data since it was felt that they all agreed within the limits of uncertainty of the data. These data suggest it is neither necessary nor prohibited to postulate that the N-terminal arms extend out from the particle. If they do, they do so at the ends and not, say, in the middle, where the shape scattering and radius of gyration would be affected in a way that is not consistent with the data on the shape of the dimer. An experiment on the cleaved dimer, or a contrast matching experiment on dimer with the lysines (which occur primarily in the N-terminal arms) labeled with deuterated methyl groups, would help clarify the locations of these parts of the histones.

Further information about the conformations of the H2a and H2b within the dimer was obtained from contrast matching studies of the reconstituted, partially deuterated dimer $(H2a)_H$-$(H2b)_D$ from Euglena. There are no appreciable, naturally occurring differences between the scattering length densities of individual histones, like those between such different classes of macromolecules as proteins, nucleic acids, and lipids. It has been possible, however, to obtain histones with artificially enhanced scattering length densities, by isolating them from Euglena grown in media containing high levels of $D_2O$. For Euglena grown in 80% $D_2O$ media, it was observed that about 50% of the nonexchanging hydrogen atoms were replaced by deuterium atoms. Calculations showed that this would result in a change in the match-point of the 50% deuterated histone from about 40% $D_2O$ to about 90%, and this was confirmed by measuring the shift in the match-point of the $(H2a)_H$-$(H2b)_D$. This is a significant difference, even larger than the natural contrast between the DNA and protein in the nucleosome. Thus, after reconstituting complexes with one of the histones deuterated, it is possible, by using contrast matching techniques, to focus on the arrangement of the individual histones. With deuterated dimers and tetramers, it should be possible to study the dimer and tetramer conformations within the octamer as well. By varying the percentage of $D_2O$ and $H_2O$ in the buffer, the contrast dependence of the radius of gyration of a partially deuterated complex can be determined, and a buffer with a scattering length density equal to that of the undeuterated protein can be chosen, so that this protein is essentially matched out. The scattering experiment on the partially deuterated dimer represents the first such contrast matching experiment on histone complexes.

The scattering profile for $(H2a)_H$-$(H2b)_D$ in 39.7% $D_2O$, near the match-point of undeuterated H2a, indicates that the H2b is itself about as asymmetric as the whole dimer, not half as much. Other data also support the conclusion that the H2a and H2b are not located as separate domains at the two ends of the dimer, but that each is elongated and they interact along the elongated axis

of the dimer. The radius of gyration of the dimer in the 39.7% $D_2O$ buffer was 17.2±0.8 Å, much larger than the value that would be obtained by cutting the various dimer models in half perpendicular to the elongated axis. Likewise, the radius of gyration in an 85.7% buffer, near the match-point of the 50% deuterated H2b, was 16.7±0.7 Å. This is equivalent to saying that the curvature of the Stuhrmann plot is less than it would be if these two histones occupied the two ends of the dimer. The calculated separation of the centers of mass of the H2a and H2b, which depends on b, the second coefficient of the quadratic equation that describes the contrast dependence of the radius of gyration, is 20 Å, much too small to be consistent with an end-to-end model. The H2a and H2b interaction must extend along the elongated axis. This may be related to the observation that there is a large change in the amount of α-helix (15 residues) when H2a and H2b are mixed to form the dimer (10).

A previous study has shown that Euglena can be grown in $D_2O$ media containing deuterated algal extracts and deuterated glucose as carbon sources (29). Growth is extremely slow (48), however, and large amounts of deuterated carbon sources would be needed for growing large batches. In the present experiments, the amount of $D_2O$ in the media was limited to 80 to 85% to maintain vigorous growth. Undeuterated glutamic and malic acids were used as carbon sources. Probably the amount of deuterium incorporated at non-exchangeable hydrogen sites and thus the scattering length density could be increased by using a deuterated carbon source but not increasing the $D_2O$ level in the media (which would slow the growth rate). For example, a good choice would be to replace the undeuterated carbon sources with $d_6$-succinic acid. Euglena has been shown to grow well when succinic acid is the sole carbon source (8), and this form can be prepared, by hydrolysis with $D_2O$, from $d_4$-succinic anhydride, which can be produced relatively simply and inexpensively in large batches (40).

Euglena has been used as a source of partially deuterated histones because higher eukaryotes can tolerate only much lower levels of $D_2O$. The efficacy of comparing data on the conformations of Euglena histone complexes with those from chicken erythrocytes is a result of the highly conservative nature of the histones. Certainly the organization of nucleosomes in Euglena chromatin is similar to that in other eukaryotes (12,28), and a set of histones similar to the core particle histones of other eukaryotes has been identified (22). We have observed that the organization of these histones in Euglena is very similar to that in other species. An octamer complex can be extracted in 2.0 M NaCl. At lower salt concentrations, sequential extraction of the H2a-H2b and $(H3\text{-}H4)_2$ complexes is possible, although this is complicated because Euglena H1 is displaced from the DNA at about the same salt concentration as the H2a-H2b. Unlike the tetramer, how-

ever, the Euglena dimer undergoes some dissociation at 0.2 M NaCl. The scattering experiments were therefore done in 2.0 M NaCl, in which the dimer is stable. We had found in previous experiments with chicken H2a-H2b (unpublished) that the scattering profiles and radii of gyration of the dimer were essentially identical in scattering buffer containing either 0.2 M or 2.0 M NaCl. We had also observed that the chicken H2a-H2b dimer formed by mixing the individual histones had the same scattering profile as the salt-extracted dimer.

## SUMMARY

Neutron scattering experiments have shown that both the $(H3\text{-}H4)_2$ and H2a-H2b histone complexes are quite asymmetric in solution. The $(H3\text{-}H4)_2$ tetramer is an oblate or flattened structure, with a radius of gyration almost as large as that of the core octamer. If the tetramer is primarily globular, it must have an axial ratio of about 1:5. It is more likely, however, that this asymmetry results in part from N-terminal arms that extend outward approximately within the major plane of the particle. If this is the case, less asymmetric models for the globular part of the tetramer, including a dislocated disk of the type proposed by Klug et al. (23), can be made consistent with the scattering data. The H2a-H2b dimer, on the other hand, is an elongated structure. The low resolution data are in good agreement with those calculated for a cylindrical model 64 x 27 Å, but other elongated models fit those data almost as well, including one that approximates free N-terminal arms at each end. Free arms are not necessary, but they must extend from the ends if they exist. A contrast matching experiment done with 50% deuterated H2b nd undeuterated H2a in the reconstituted dimer showed that these two histones must each be rather elongated within the complex and are not just confined to one end. The amount of scattering contrast between the undeuterated and 50% deuterated histones was sufficient to suggest further experiments using complexes reconstituted from mixtures of undeuterated and partially deuterated histones which will help elucidate their arrangement within the histone complexes and within the octamer core of the nucleosome core particle.

## ACKNOWLEDGMENTS

The author wishes to thank Teresa Kelley and Susan S. Lamm for their excellent technical assistance, and Susan S. Lamm for aid in preparation of the manuscript. He is also indebted to Nicholas Alonzo for making amino acid composition measurements and to Dr. Alan C. McLaughlin for measuring the proton NMR spectra.

REFERENCES


1. Beaudette, N.V., Fulmer, A.W., Okabayashi, H., and Fasman, G.D., Biochemistry 20:6526 (1981).
2. Beeman, W., Kaesberg, P., Anderegg, J.W., and Webb, M.B., Handb. Phys. 32:321 (1957).
3. Bohm, L., Hayashi, H., Cary, P.D., Moss, T., Crane-Robinson, C., and Bradbury, E.M., Eur J. Biochem. 77:487 (1977).
4. Bolund, L. and Johns, E.W., Eur. J. Biochem. 35:546 (1973).
5. Bonner, W.M. and Pollard, H.B., Biochem. Biophys. Res. Commun. 64:282 (1975).
6. Bradbury, E.M., Ciba Found. Symp. 28:131 (1975).
7. Brandt, W.F. and von Holt, C., Eur. J. Biochem. 46:419 (1974).
8. Cramer, M. and Myers, J., Arch. Mikrobiol. 17:384 (1952).
9. Crespi, H.L. and Katz, J.J., Anal. Biochem. 2:274 (1961).
10. D'Anna, J.A.D. Jr. and Isenberg, I., Biochemistry 13:4992 (1974).
11. Debye, P., Ann. Physik 43:49 (1915).
12. Delpech, S., Bre, M.H., Mazen, A., deMurcia G., Champagne, M., and Lefort-Tran, M., Cell Biol. Int. Rep. 6:197 (1982).
13. Eickbush, T.H. and Moudrianakis, E.N., Biochemistry 17:4955 (1978).
14. Finch, J.T., Lutter, L.C., Rhodes, D., Brown, R.S., Rushton, B., Levitt, M., and Klug, A., Nature 269:29 (1977).
15. Hewish, D.R. and Burgoyne, L.A., Biochem. Biophys. Res. Commun. 52:504 (1973).
16. Hjelm, R.P., Kneale, G.G., Suan, P., Baldwin, J.P., and Bradbury, E.M., Cell 10:139 (1977).
17. Hutner, S.H., Zahalsky, A.C., Aaronson, S., Baker, H., and Frank O., Methods Cell Physiol. 2:217 (1966).
18. Ibel K. and Stuhrmann, H.B., J. Mol. Biol. 93:255 (1975).
19. Isenberg, I., in: "Search and Discovery. A Tribute to Albert Szent-Gyorgyi," B. Kaminer, ed., pp. 195-215, Academic Press, New York (1977).
20. Isenberg, I., Annu. Rev. Biochem. 48:159 (1979).
21. Jacrot, B., Rep. Prog. Phys. 39:911 (1976).
22. Jardine, N.J. and Leaver, J.L., Biochem. J. 169:103 (1978).
23. Klug, A., Rhodes, D., Smith, J., Finch, J.T., and Thomas, J.O., Nature 287:509 (1980).
24. Kratky, O. and Pilz, I., Q. Rev. Biophys. 5:481 (1972).
25. Laine, B., Kmiecik, D., Sautiere, P., and Biserte, G., Biochimie 60:147 (1978).
26. Lattman, E., Burlingame, R., Hatch, C., and Moudrianakis, E.N., Science 216:1016 (1982).
27. Magnaval, R., Bertaux, O., and Valencia, R., Exp. Cell Res. 121:251 (1979).
28. Magnaval, R., Valencia, R., and Paoletti, J., Biochem. Biophys. Res. Commun. 92:1415 (1980).

29. Mandeville, S.E., Crespi, H.L., and Katz, J.J., Science 146:769 (1964).
30. Martinson, H.G., Shetlar, M.D., and McCarthy, B.J., Biochemistry 15:2002 (1976).
31. Moore, P.B., Anal. Biochem. 82:101 (1977).
32. Moss, T., Cary, P.D., Crane-Robinson, C., and Bradbury, E.M., Biochemistry 15:2261 (1976).
33. Moss, T., Cary, P.D., Abercrombie, B.D., Crane-Robinson, C., and Bradbury, E.M., Eur. J. Biochem. 71:337 (1976).
34. McGhee, J.D. and Felsenfeld, G., Annu. Rev. Biochem. 49:1115 (1980).
35. Pardon, J.F., Worcester, D.L., Wooley, J.C., Cotter, R.I., Lilley, D.M.J., and Richards, B.M., Nucleic Acids Res. 4:3199 (1977).
36. Roark, D.E., Geoghegan, T.E., Keller, G.H., Matter, K.V., and Engle, R.L., Biochemistry 15:3019 (1976).
37. Schneider, D.K. and Schoenborn, B.P., See paper in this Symposium.
38. Schoenborn, B.P., Alberi, J., Saxena, A.M., and Fischer, J., J. Appl. Crystallogr. 11:455 (1978).
39. Simon, R.H. and Felsenfeld, G., Nucleic Acids Res. 6:689 (1979).
40. Stella, V.J., J. Pharm. Sci. 62:634 (1973).
41. Suau, P., Kneale, G.G., Braddock, G.W., Baldwin, J.P., and Bradbury, E.M., Nucleic Acids Res. 4:3769 (1977).
42. Thomas, J.O. and Butler, P.J.G., Cold Spring Harbor Symp. Quant. Biol. 42:119 (1977).
43. van der Westhuyzen, D.R., Bohm, E.L., and von Holt, C., Biochim. Biophys. Acta 359:341 (1974).
44. Van Helden, P.D., Strickland, W.N., Strickland, M., and von Holt, C., Biochim. Biophys. Acta 703:17 (1982).
45. von Holt, C., Strickland, W.N., Brandt, W.F., and Strickland, M.S., FEBS Lett. 100:201 (1979).
46. Wise, D.S., Karlin, A., and Schoenborn, B.P., Biophys. J. 28:473 (1979).
47. Mardian, J.K.W. and Olins, D.E. (Oak Ridge National Laboratory), Personal communication (1981).
48. Crespi, H.L. (Argonne National Laboratory), Personal communication (1979).

## DISCUSSION

MENDELSON: Were the electron microscopy image reconstruction models scaled to give the proper volume for comparison with your scattering data? If so, how was this done?

CARLSON: The actual dimensions of a model are not important in a plot of ln[I/I(0)] versus ln(QR), only the shape. Once the shape is specified, the dimensions are chosen to attempt to optimize agreement between the radius of gyration and the volume.

ZACCAI: Considering the charged nature of the protein, is it not surprising that you saw no interparticle effect up to concentrations of 20 mg/ml? Could you remind me of the salt concentration in the buffer?

CARLSON: The individual histones show a much more pronounced tendency to aggregate than do the pair complexes. Neither the dimers nor the tetramers aggregate in scattering buffer containing 0.2 M NaCl. There was no significant concentration dependence from about 2 to 20 mg/ml. When the NaCl concentration is increased to 2.0 M, the dimers still do not form larger aggregates, but the tetramers do. A mixture of dimers and tetramers, separable in 0.2 M NaCl buffer, also associates to form the octamer in 2.0 M NaCl. The histones are highly basic (the ratio of positively to negatively charged amino acids is about 3:1), and the charged amino acids are distributed very asymmetrically. It may be that the formation of a pair complex blocks most negatively charged groups. Then the electrostatic forces between pairs are primarily repulsive. When the salt concentration is increased to the point that these are electrostatically shielded, association can occur. I have observed that when the extremely positive charged N-terminal arms of the tetramer are cleaved off with trypsin, serious aggregation problems develop, even at the lower salt concentration.

ZACCAI: In the Stuhrmann plot ($R^2$ vs $1/\bar{\rho}$), why are the $R_o$ different in the two cases, (H-H), (H-D) for the H2a-H2b dimer?

CARLSON: There is a difference of about 5% in the $R_o$, the radii of gyration at infinite contrast. This may indicate that there is a small difference between the structures of Euglena and chicken dimers, or it may be due to a systematic error arising because the experiments were done on different low-angle spectrometers.

MAY: How do you explain the discrepancies between the volume in the ellipsoidal model and the volume calculated from I(0)?

CARLSON: I am sure that the ellipsoidal model does not accurately describe the tetramer, but it does indicate how asymmetric the actual structure must be. There is evidence that the structure has a central hole and that it is only partially globular, so it may be a more open structure.

## DISCLAIMER